Available online at www.sciencedirect.com

ScienceDirect

Procedia Manufacturing 47 (2020) 713–718

Procedia MANUFACTURING

www.elsevier.com/locate/procedia

23rd International Conference on Material Forming (ESAFORM 2020)

Virtual Element Method for Cross-Wedge Rolling during Tailored Forming Processes

Christoph Böhm[a,*], Jens Kruse[b], Malte Stonis[b], Fadi Aldakheel[a], Peter Wriggers[a]

[a]*Institute of Continuum Mechanics, Leibniz University Hannover, Appelstraße 11, 30167 Hannover, Germany*
[b]*Institut für Integrierte Produktion Hannover gGmbH, Hollerithallee 6, 30419 Hannover, Germany*

* Corresponding author. Tel.: +49 511.762-19057; fax: +49 511.762-5496. *E-mail address:* boehm@ikm.uni-hannover.de

Abstract

In this work we present an application of the virtual element method (VEM) to a forming process of hybrid metallic structures by cross-wedge rolling. The modeling of that process is embedded in a thermomechanical framework undergoing large deformations, as outlined in [1, 2]. Since forming processes include mostly huge displacements within a plastic regime, the difficulty of an accurate numerical treatment arises. As shown in [3], VEM illustrates a stable, robust and quadratic convergence rate under extreme loading conditions in many fields of numerical mechanics. Numerically, the forming process is achieved by assigning time-dependent boundary conditions instead of modeling the contact mechanics yielding to a simplified formulation. Based on the two metallic combinations of steel and aluminum, different material properties are considered in the simulations. The purpose of this contribution is to illustrate the effectiveness of such a non-contact macroscopic framework by employing suitable boundary conditions within a virtual element scheme. A comparison with the classical finite element method (FEM) is performed to demonstrate the efficiency of the chosen approach. The numerical examples proposed in this work stem out from the DFG Collaborative Research Centre (CRC) 1153 “Process chain for the production of hybrid high-performance components through tailored forming”.

© 2020 The Authors. Published by Elsevier Ltd.
This is an open access article under the CC BY-NC-ND license (https://creativecommons.org/licenses/by-nc-nd/4.0/)
Peer-review under responsibility of the scientific committee of the 23rd International Conference on Material Forming.

Keywords: Virtual Element Method (VEM); Tailored Forming; Cross Wedge Rolling; Large Deformations

1. Introduction

Over many years, simulative predictions of forming processes have been established by using a physical modeling embedded in a numerical framework. This treatment is used within the design and the development process of industrial applications. As an output the amount of experiments decreased. Hence using simulations to e.g. optimize process parameters with respect to certain requirements of the results can reduce both, the amount of costs and time. As a consequence, the requirement of an accurate treatment within this numerical framework arises. The simulations of forming processes are mostly done in finite element method (FEM) environments. The accuracy of those simulations is mainly influenced by two parts. On the one hand, the modeling of the material behavior has to be in line with the first and the second law of thermodynamics, as documented in [1], to hold the thermodynamic consistency in terms of entropy. On the other hand, inelastic deformations during the forming processes are limited, hence numerical treatments of the developed models are approximations. This implies a necessity of using accurate schemes and element definitions. As outlined in [3] and especially in [2], the virtual element method (VEM) has shown both, robustness and accuracy, in comparison to FEM. In particular, VEM demonstrated advantages in processes with large deformations and a thermomechanical coupling, [2, 3]. Furthermore, VEM is a competitive discretization scheme for meshes with highly irregular shaped elements. Recent works on virtual elements have been devoted to linear elastic deformations in [4, 5], contact problems [6], anisotropic

2351-9789 © 2020 The Authors. Published by Elsevier Ltd.
This is an open access article under the CC BY-NC-ND license (https://creativecommons.org/licenses/by-nc-nd/4.0/)
Peer-review under responsibility of the scientific committee of the 23rd International Conference on Material Forming.
10.1016/j.promfg.2020.04.220

materials in [7, 8], inelastic solids in [9], crack-propagation for 2D elastic solids at small strains in [10] and curvilinear virtual elements for 2D solid mechanics applications in [11]. Recently, [12, 13] propose an efficient virtual element scheme for the phase-field modeling of brittle and ductile fracture. By combining this, VEM is an attractive method for simulative predictions of forming processes instead of a classical finite element framework.

This paper extends VEM towards industrial applications by modeling the cross-wedge rolling processes numerically.

Nomenclature

$\boldsymbol{C}$	right Cauchy Green tensor
$\boldsymbol{F}$	gradient of deformation
$\boldsymbol{n}$	vector normal to elastic region
$\boldsymbol{s}$	deviatoric stress
$\boldsymbol{u}$	displacement
$\mathbb{A}$	local tangent operator
$\mathcal{H}$	history field
$\mathfrak{H}$	array of primary fields
$\mathcal{R}$	local residual in the plastic routine
α	equivalent plastic strain
β	stabilization parameter
ϑ	temperature
ϕ	flow rule
ψ	thermodynamic potential

2. Tailored Forming

Due to the rising demand of lightweight components and functionality, new innovative processes and chains have to be developed. In industrial process chains the forming is mostly done before joining the individual parts [14, 15]. The process chain "tailored forming" advances this order and does the forming after a joining of two or more individual parts, as shown in Fig. 1.

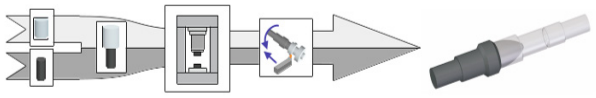

Fig. 1. Process chain "Tailored Forming" for joining, forming and finishing a shaft, made out of two different metallic monomaterials.

As a result, complex shaped hybrid structures can be produced. Another aspect of modifying the established process chains is the steadily increasing request for a certain material response at different locations of the structure [14]. As an example, the highly loaded layer in a hybrid bearing bush has to be more strength than the material far away from the contact zone [16].

The combination of two or more materials for reaching higher adaption of locally material behavior could also be extended to shafts and gears, as outlined in [17, 18]. Due to the combination of individual metallic materials, like aluminum and steel, arise multiple issues. Since different materials have unequal yield strength or temperature behavior, the forming process gains more difficulty. The primary objective of the Collaborative Research Centre 1153 (CRC 1153) is to investigate the scientific questions emerged from the new process chain tailored forming. This includes the joining as well as forming and heat treatments up to finishing. Within this CRC 1153, subproject C4 "Intermediate Layer Modelling" models the material behavior of these structures on both, microstructural and macrostructural level [17, 19, 20]. Furthermore, C4 investigates also the numerical treatment of the developed models, as outlined in [1, 2, 3]. Within the new process chain tailored forming a numerical study of material behavior during forming processes will help other subprojects at obtaining suitable parameters for their processes.

3. Thermo-Elasto-Plasticity at Finite Strains

Since the yield strength of hybrid structures is different at each individual part, a heat treatment has to ensure an adjustment of it. Hence a thermo-mechanical coupling exists. Furthermore, huge plastic deformations during the forming processes were observed. Thus, extending the model towards finite strain plasticity is required. To this end, the coupled problem is characterized by two primary fields, namely the displacement $\boldsymbol{u}$ and the temperature field ϑ, see [21, 22, 23]. In line with [1], the kinematics contain a multiplicative elastic-plastic split of the gradient of deformation. This split describes the large deformations by including plasticity [1, 33]. Metallic materials behave almost isochoric at a plastic range [24]. Hence an isochoric von Mises J_2-plasticity model is chosen for the flow rule ϕ. As a consequence, the determinant of the plastic part of $\boldsymbol{F}$ has to be equal to one at every step, which implies that the Jacobian J is only influenced by its elastic part [1]. The heat transfer is covered by a Fourier-type law, as outlined in [1, 25, 26, 33]. The elastic work, stored in the components, is governed by a thermodynamic potential ψ. In line with [1], this potential is split into a pure thermal part and a thermo-elastic coupled part. Moreover ψ contains also volumetric and isochoric parts of the pure elastic energy, as well as a plastic potential which accounts for softening and hardening effects by considering temperature changes. The setup for the evolution equations of the plastic variables is covered by an exponential map, as illustrated in [1, 27],

$$\boldsymbol{C}_p^{-1} = \exp(-2\Delta\alpha \boldsymbol{F}^{-1}\boldsymbol{n}\boldsymbol{F})\boldsymbol{C}_{p,n}^{-1}. \tag{1}$$

Following [1, 27], the normal vector $\boldsymbol{n}$ is obtained by taking the derivative of the flow rule ϕ with respect to the deviatoric stress

$$\boldsymbol{n} = \partial_{\boldsymbol{s}}\phi. \tag{2}$$

With that at hands, the history field $\mathcal{H} := \{\boldsymbol{C}_p^{-1}, \alpha\}$ can be updated by the following routine [27].

Table 1. Routine for obtaining $\mathcal{H}$ at current time step.

Find: $\mathcal{H}$	Given: $\mathcal{H}_n, \boldsymbol{F}$
Kinematics	
• Compute deformation measure	

• Compute invariants
Constitutive equations
• Calculate ψ
• Obtain stress measure
Elastic trial
• Evaluate ϕ
○ $\phi < 0 \rightarrow \mathcal{H} = \mathcal{H}_n$, else: Compute $\boldsymbol{s}$ & $\boldsymbol{n}$
Plastic step
• Find $\Delta\mathcal{H}$ by minimization of the local residual $\mathcal{R}$

When the yield criterion is reached and plasticity occurs, the elastic region is also adapted in line with the history field at the current time step. Hence a stiffening or a softening could take place [1]. The local residual $\mathcal{R}$ in table 1 is an array and contains seven independent entries [27], where six refer to the exponential map and the left entry is the flow rule ϕ. Hence a set of nonlinear equations has to be solved in terms of computing $\mathcal{H}$ at the current step. By using the software package *AceGen*, which can perform such computations by automatic derivation of the primal problem [28], it can be written as follows

$$\mathbb{A}\Delta\mathcal{H} + \mathcal{R} = \mathbf{0}, \;\; \mathbb{A} = \partial_{\mathcal{H}}\mathcal{R}. \tag{3}$$

With the local tangent operator $\mathbb{A}$ at hands, the set of equations for obtain the new history field can be solved by perform a *Newton-Raphson iteration procedure* [28]. The described scheme is locally embedded within a global routine for solving the discretized set of coupled equations [1].

4. Virtual Element Method

There are many methods existing for a numerical treatment of physical problems in both, science and applications. Methods like finite difference schemes or finite element schemes have wide range of specializations and have been applied to many different problems in the last decades. Thus, many varying formulations existing and there are many developments within the schemes, for instance the extended finite element method for fracture mechanics [3]. Hence special knowledge for the use of this formulations and for the modelling of the physics is necessary. By applying such discretization schemes to an inadequate problem formulation, the methods can lead to inadequate results, too. However, there is still a wide range of possible advancement within this field. One new and recent developed method is the virtual element method (VEM). The method was developed by F. Brezzi and coworkers in [4, 5].

Virtual elements can be of arbitrary shape, incorporating also non-convex shaped geometries, see in Fig. 2. As a result, the number of nodes could differ between the individual virtual elements. In line with [1] the primary fields are split into a *projection part* $\mathfrak{H}_\pi := \{\boldsymbol{u}_\pi, \vartheta_\pi\}$ and a remainder

$$\mathfrak{H} = \mathfrak{H}_\pi + (\mathfrak{H} - \mathfrak{H}_\pi). \tag{4}$$

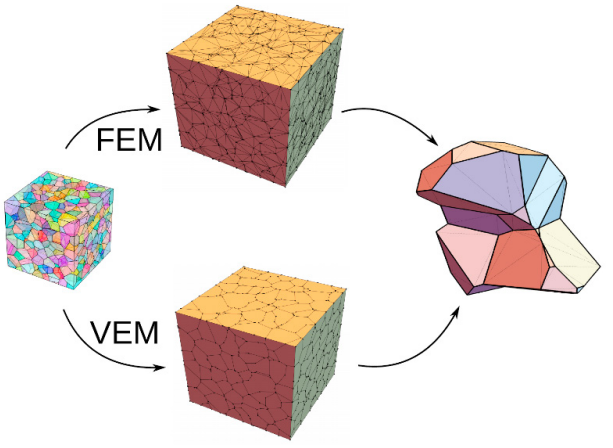

Fig. 2. Discretization of a 3D cube, made out of non-convex polygons, by linear tetrahedral elements (top) and virtual elements (bottom). Non-convex grain with VE-discretization & FE-submesh (triangles, dashed lines).

Thus, the *projection* is calculated by making an ansatz regarding the total primary field, as outlined in [1]. The equation set for the primary field, shown in eq. (4), is evaluated at the boundaries of each virtual element [1]. Following [1, 2, 3], the defined potential is also split up into a stabilization term and a compatibility part. The local routine for obtaining the new history field, described in Table 1 and eq. (3), is evaluated at the centroid of each virtual element [1]. The impact of the stabilization is controlled by a *stabilization parameter* β_i for each primary field [1, 2, 3].

The formulation of the continuum mechanics and the element routine is derived within the symbolic mathematic software tool *AceGen* [28]. The numerical studies are done within the corresponding finite element environment *AceFEM* [28].

To illustrate the performance of the proposed virtual element formulation for modeling finite strain thermo-elasto-plastic problems, we investigate the necking phenomenon in a bar due to prescribed displacement along axial direction, as outlined [1, 22, 23]. Fig. 3 depicts the evolution of the equivalent plastic strain α for steel specimen at different stages of deformations using VEM-VO mesh. We notice huge plastic deformations as a necking zone and heat concentration at the center of the bar. Similar results are also observed for Aluminum specimen, due to that we omit plotting it.

In future work, the within the chapter 5 described experimental cross-wedge rolling process will be modelled with the VEM. Currently the process is simulated with FEM within the software Transvalor Forge NxT 3.0.

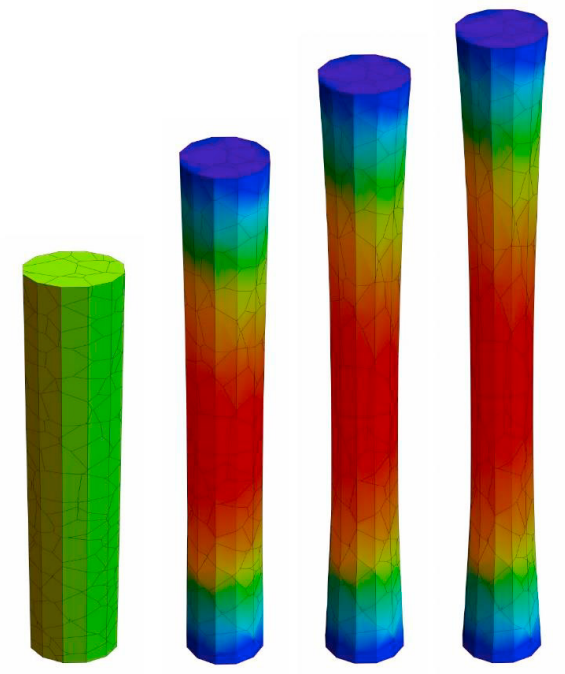

Fig. 3. Uniaxial tension test of a monomaterial bar, discretized by a VEM-VO mesh. Contour plot of the equivalent plastic strain α evolution.

5. Experimental Cross-Wedge Rolling Setup

Cross-Wedge Rolling (CWR) is a common manufacturing technology, manly used for creating preforms for forging operations, like die forging [29]. The process of CWR starts with an, usually cylindric, billet, formed between two moving tools. The CWR tools can be shaped as round tool design or flat tool design [29]. Within the subproject B1 of the CRC 1153, a test stand in flat tool design is used. Each CWR tool holds at least one wedge on its surface, responsible for displacing the material axially. Therefore, the tools are moving translatorial to each other, see Fig. 4 (a). The tools used to create the demonstrator parts shaft 1 and shaft 3 of the CRC consist of six wedges, each. The total length of the tools is 1500 mm, the width 250 mm. The lower tool is shown in Fig. 4 (b).

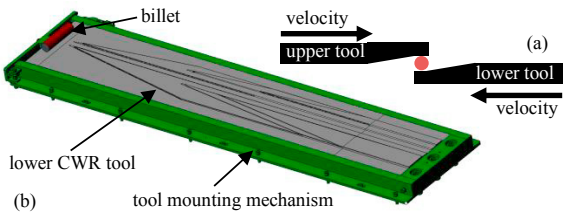

Fig. 4. (a) Process kinematic; (a) Lower Cross-Wedge Rolling tool.

Shaft 1 is made from coaxially arranged billets (Fig. 5), shaft 3 is made from serially arranged billets (Fig. 6). Shaft 3, made of aluminium and steel, has a large light-weight potential (more than 30 % mass reduction compared to a full steel shaft). Shaft 1 has the potential to combine hard facing alloys with durable ductile steels to improve part life time [30].

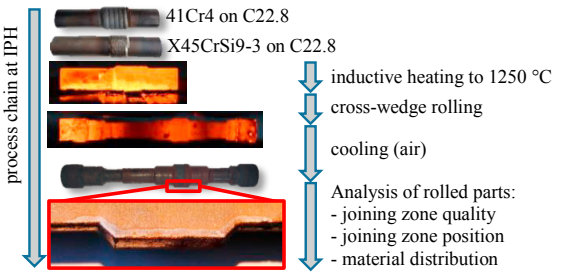

Fig. 5. Process chain of shaft 1 made of steel.

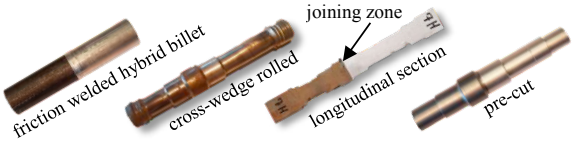

Fig. 6. Process chain of shaft 3 made of aluminium and steel.

Depending on the material combination used for CWR, the heating strategy is adapted: Hybrid billets consisting of different steel grade alloys are heated homogenously to 1250 °C [30, 31] - hybrid billets made of aluminium and steel are inhomogeneously heated [32]. The billets are heated via induction heating. In case of the aluminium-steel combination, only the steel part of the billet is heated, see Fig. 7 (a). The thermal energy is then transported via thermal conduction from the steel part into the aluminium part of the billet. The amount of heating power induced into the billet and the duration of the heating determines the temperature gradient within the billet. Fig. 7 (b) shows the currently used starting thermal distribution for aluminium-steel billets after heating, when rolling shaft 3 [32].

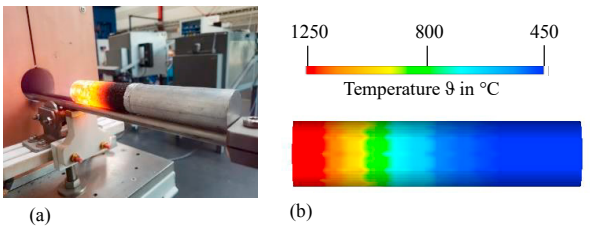

Fig. 7. (a) Inhomogeneous heating; (b) Temperature distribution after heating.

After heating, the billets are – currently manually – inserted into the CWR test stand. The position of the billet with regard to the first wedge insertions depends on the type of billet: coaxially arranged billets are placed with the welded-on material between the two main wedges. Between these wedges, the bearing seat of the shaft is formed. Combined aluminium-steel billets are positioned with the

joining zone out of the area of the bearing seat, which is supposed to be steel only after rolling (compare Fig. 6).

Speed, friction and heat transfer between billet and tools have large impact on the quality of the rolled part [29]. To ensure rolling without slipping or sliding, serrations are implemented within the shoulders of the tool wedges. The friction coefficient (in the simulation software Forge NxT by Transvalor, the Tresca friction model with m = 0.8 to 1.0 is used [29]) depends on the surface quality of the billets and the tools and the materials used. Especially during hot forming (1250 °C initial billet temperature), scale and heat transfer influence the friction between tool and billet.

Each of the two tools is moved by one hydraulic cylinder, capable of a maximum force of 125 kN. The forces necessary to keep a constant rolling gap during forming are provided by a hydraulic press, into which the CWR test stand is mounted. Even though the press provides up to 6300 kN, not more than times 4 of the horizontal forming forces has been encountered during rolling the shaft geometry – therefore 500 kN of "closing force" are sufficient. The initial speed of each tool is 150 mm/s. When forming forces reach the maximum of 125 kN, speed decreases to ensure not exaggerating the maximum allowed pressure of the hydraulic system.

Acknowledgements

The authors want to acknowledge the Deutsche Forschungsgemeinschaft (DFG) with the Collaborative Research Center 1153 (CRC 1153) "Process chain for the production of hybrid high-performance components through tailored forming". The results presented in this work were obtained by a cooperation between the subprojects C4 and B1 within the CRC 1153.

References

[1] Aldakheel F, Hudobivnik B, Wriggers P. Virtual elements for finite thermo-plasticity problems. Computational Mechanics 2019;64 (5); 1347–1360.

[2] Hudobivnik B, Aldakheel F, Wriggers P. A low order 3D virtual element formulation for finite elasto-plastic deformations. Computational Methods 2019;63 (2); 253–269.

[3] Wriggers P, Aldakheel F, Hudobivnik B. Application of the Virtual Element Method in Mechanics. GAMM Rundbrief 01/2019.

[4] Beirão Da Veiga L, Brezzi F, Cangiani A, Manzini G, Marini LD, Russo A. Basic principles of virtual element methods. Mathematical Models and Methods in Applied Sciences 2013;23; 199-214.

[5] Beirão Da Veiga L, Brezzi F, Marini LD. Virtual Elements for linear elasticity problem. SIAM Journal of Numerical Analysis 2013;51 (2); 794-812.

[6] Wriggers P, Rust WT, Reddy BD. A virtual element method for contact. Computational Mechanics 2016; 58 (6); 1039-1050.

[7] Wriggers P, Hudobivnik B, Schröder J. Finite and Virtual Element Formulations for Large Strain Anisotropic Material with Inextensive Fibers. Multiscale Modeling of Heterogeneous Structures 2018; 205-231.

[8] Reddy BD, van Huyssteen DA. virtual element method for transversely isotropic elasticity. Computational Mechanics 2019;64 (4); 971-988.

[9] Taylor RL, Artioli E. VEM for Inelastic Solids. Advances in Computational Plasticity 2018; 381-394.

[10] Hussein A, Aldakheel F, Hudobivnik B, Wriggers P, Guidault PA, Allix O. A computational framework for brittle crack-propagation based on efficient virtual element method. Finite Elements in Analysis and Design 2019;159; 15-32.

[11] Artioli E, Beirão Da Veiga L, Dassi F. Curvilinear Virtual Elements for 2D solid mechanics applications. Computer Methods in Applied Mechanics and Engineering 2019;112667.

[12] Aldakheel F, Hudobivnik B, Hussein A, Wriggers P. Phase-Field Modeling of Brittle Fracture Using an Efficient Virtual Element Scheme. Computer Methods in Applied Mechanics and Engineering 2018;341; 443-466.

[13] Aldakheel F, Hudobivnik B, Wriggers P. Virtual element formulation for phase-field modeling of ductile fracture. International Journal for Multiscale Computational Engineering 2019;17 (2); 181-200.

[14] Blohm T, Nothdurft S, Mildebrath M, Ohrdes H, Richter J, Stonis M, Langner J, Springer A, Kaierle S, Hassel T, Wallaschek J, Overmeyer L, Behrens BA. Investigation of the joining zone of laser welded and cross wedge rolled hybrid parts. International Journal of Material Forming 2018;11 (6); 829–837.

[15] Blohm T, Langner J, Stonis M, Behrens BA. Basic study of incremental forming of serially arranged hybrid parts using cross-wedge rolling. Procedia Engineering 2017;207; 1677-1682.

[16] Behrens BA, Chugreev A, Matthias T, Poll G, Pape F et al. Manufacturing and Evaluation of Multi-Material Axial-Bearing Washers by Tailored Forming. Metals 2019;9 (2):232.

[17] Behrens BA, Breidenstein B, Duran D, Herbst S, Lachmayer R, Löhnert S, Matthias T, Mozgova I, Nürnberger F, Prasanthan V, Siqueira R, Töller F, Wriggers P. Simulation-Aided Process Chain Design for the Manufacturing of Hybrid Shafts. HTM Journal of Heat Treatment and Materials 2019;74 (2); 115-135.

[18] Chugreeva A, Mildebrath M, Diefenbach J, Barroi A, Lammers M et al. Manufacturing of High-Performance Bi-Metal Bevel Gears by Combined Deposition Welding and Forging. Metals 2018;8 (11):898.

[19] Baldrich M, Aldakheel F, Beese S, Löhnert S, Wriggers P. A micro-thermo-mechanical model for a tailored formed joining zone deformed by die forging. AIP Conference Proceedings 2019;2113:0040024.

[20] Zeller S,Baldrich M, Gerstein G, Nuernberger F, Loehnert S, Maier HJ, Wriggers P. Material models for the thermoplastic material behaviour of a dual-phase steel on a microscopic and a macroscopic length scale. Journal of the Mechanics and Physics of Solids 2019;129; 205-228.

[21] Aldakheel F. Mechanics of Nonlocal Dissipative Solids: Gradient Plasticity and Phase Field Modeling of Ductile Fracture. PhD Thesis, Institute of Applied Mechanics (CE), Chair I, University of Stuttgart, 2016.

[22] Aldakheel F, Miehe C. Coupled thermomechanical response of gradient plasticity. International Journal of Plasticity 2017;91; 1-24.

[23] Aldakheel F. Micromorphic approach for gradient-extended thermo-elastic-plastic solids in the logarithmic strain space. Continuum Mechanics and Thermodynamics 2017; 29 (6); 1207-1217.

[24] Wriggers P. Nonlinear Finite Element Methods. Springer Science & Business Media 2008.

[25] Dittmann M, Aldakheel F, Schulte J, Schmidt F, Krüger M, Wriggers P, Hesch C. Phase-field modeling of porous-ductile fracture in non-linear thermo-elasto-plastic solids. Computer Methods in Applied Mechanics and Engineering 2019;112730.

[26] Krüger M, Dittmann M, Aldakheel F, Härtel A, Wriggers P, Hesch C. Porous-ductile fracture in thermo-elasto-plastic solids with contact applications. Computational Mechanics 2019; 1-26.

[27] Korelc J, Stupkiewicz S. Closed-form matrix exponential and its application in finite-strain plasticity. International Journal for Numerical Methods in Engineering 2014; 98 (13); 960-987.

[28] Korelc J, Wriggers P. Automation of Finite Element Methods. Springer International Publishing Switzerland 2016.

[29] Pater Z. 3.10 - Cross-Wedge Rolling. In: Hashmi S, Batalha GF, Van Tyne CJ, Yilbas B, editors. Comprehensive Materials Processing 2014, (3), Amsterdam: Elsevier; 211-279.

[30] Kruse J, Mildebrath M, Behrens BA, Stonis M, Hassel T. Cross-wedge rolling of PTA-welded hybrid steel billets with rolling bearing steel and hard material coatings. AIP Conference Proceedings 2019;2113:040019.

[31] Quentin L, Kruse J, Beermann R, Reinke C, Langner J, Stonis M, Kästner M, Reithmeier E. Analysis of mapped temperature data on geometry points to characterize the influence of temperature deviations on cross-wedge rolling. AIP Conference Proceedings 2019; 2113:40018.

[32] Kruse J, Jagodzinski A, Langner J, Stonis M, Behrens BA. Investigation of the joining zone displacement of cross-wedge rolled serially arranged hybrid parts. International Journal of Material Forming 2019.

[33] Aldakheel F, Mauthe S, Miehe C. Towards Phase Field Modeling of Ductile Fracture in Gradient-Extended Elastic-Plastic Solids. Proceedings in Applied Mathematics and Mechanics 2014;14 (1); 411-412.